Supplement 1

Robustness of results and representativeness of ERA5 in the vicinity of Barbados during EUREC^{4}A

This supplement addresses the robustness of the results in space and time and provides additional comparisons between ERA5 and in-situ or remote measurement data sets.

Sensitivity of transport diagnostics: The effect of the time step before arrival at which the transport diagnostics (shown in Fig. 4 of the paper) are extracted is demonstrated in Fig. S1.1. The number of air parcels with a certain characteristics strongly depends on the time step considered.

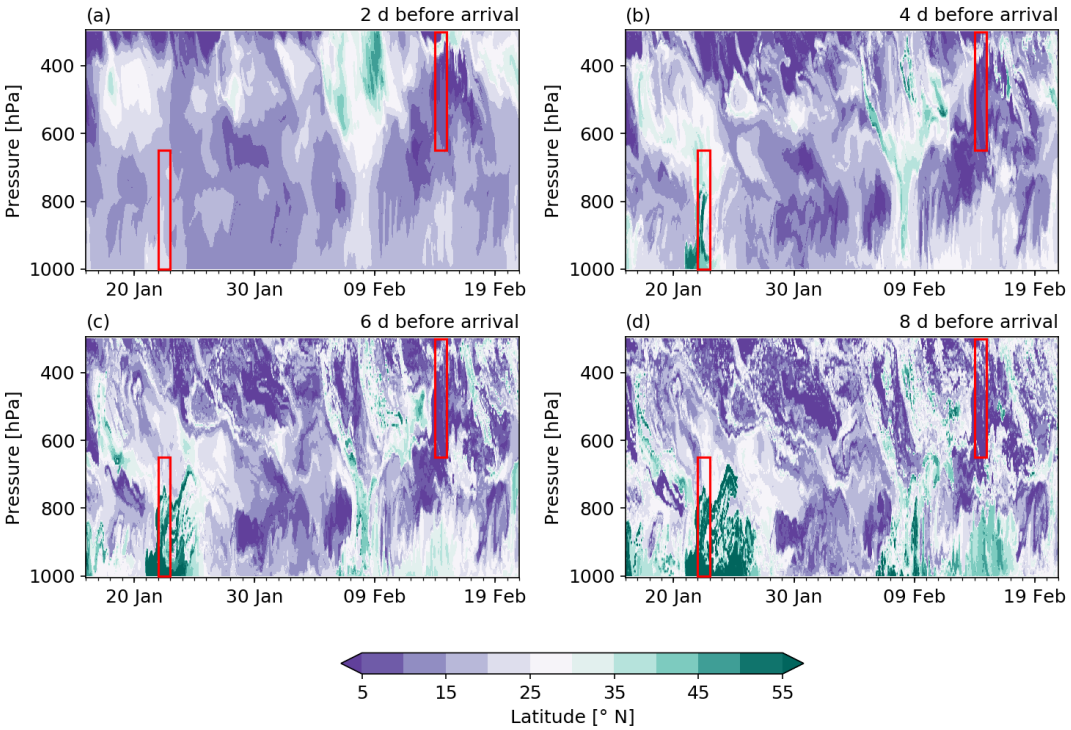

Figure S1.1: Time series of vertical profiles of the transport conditions at the BCO from 16 January to 20 February 2020. Shown is the latitudinal position of the backward trajectories started from the BCO **(a)** 2, **(b)** 4, **(c)** 6, and **(d)** 8 d before arrival. The red boxes indicate the two case studies 22 January and 14 February 2020. Data: ERA5.

Sensitivity of EDI and TMD selection: Several thresholds are defined for the identification of EDI and TMD days in the quasi-climatological period. In Fig. S1.2 the sensitivity to these definitions of the EDI/TMD occurrence frequency is shown. The number of EDIs increases substantially if a longer time span before arrival is considered (Fig. S1.2a). 22 January 2020 is identified as EDI for the range of eight to two days before arrival. If the threshold is set to two days before arrival, only four EDI cases are identified, which all lead to dry anomalies, as the air parcels have no time to pick up moisture. A change of the percentage of trajectories which need to fulfill the EDI criteria affects the EDI occurrence frequency, but the two contrasting impacts of EDIs (dry vs. moist anomaly in the layer 1000-650 hPa) always occur (Fig. S1.2b). For TMDs the events are more strongly related with moist anomalies in the layer 650-300 hPa the higher the required percentage of TMD trajectories per day is (Fig. S1.2c).

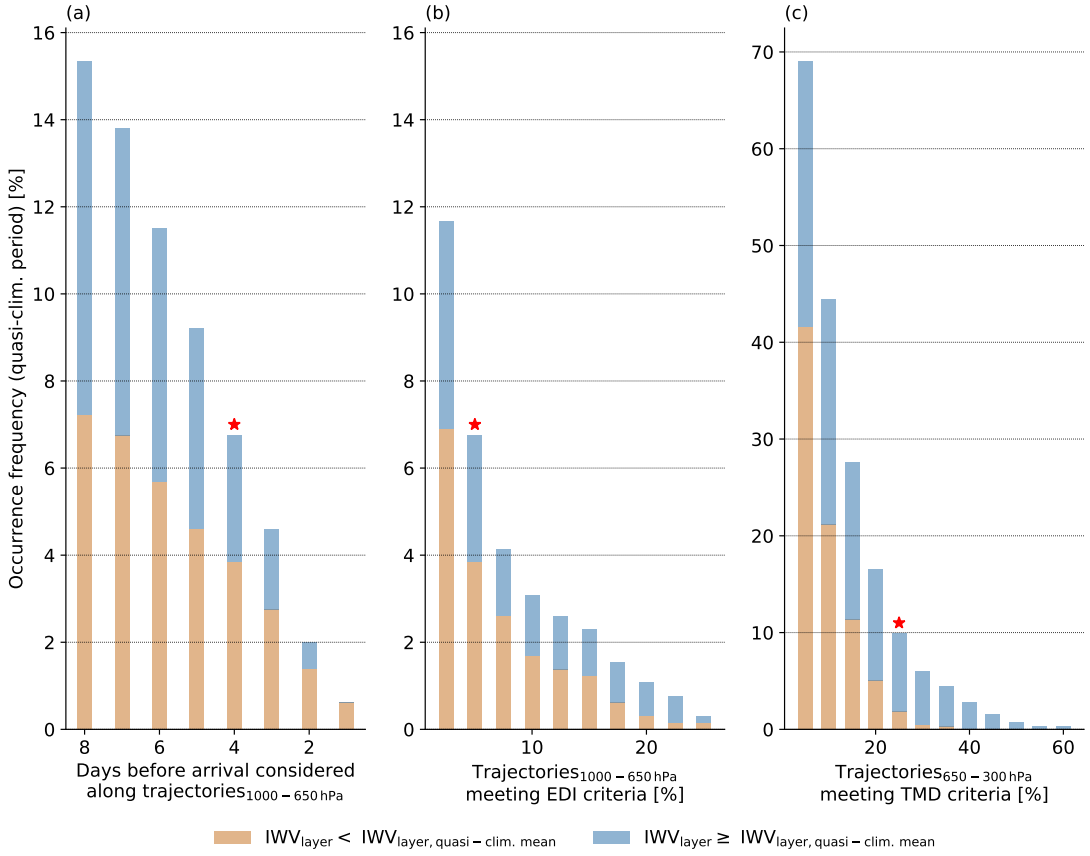

Figure S1.2: The effect of different **(a,b)** EDI and **(c)** TMD selection criteria on the occurrence frequency and the associated anomaly in IWV in Barbados. Shown are **(a)** the effect of the considered time span along the backward trajectories (started in the layer 1000-650 hPa) in which the EDI criteria need to be fulfilled, **(b,c)** the effect of the percentage of trajectories (arriving each day in the respective layer), which need to meet the criteria for identifying an EDI or TMD. The red stars indicate the threshold definition as applied in the paper, the remaining thresholds are **(a)** 5 % trajectories with a minimal descent of 400 hPa $(48\,\mathrm{h})^{-2}$ in the given time span, **(b)** a given percentage of trajectories with a minimal descent of 400 hPa $(48\,\mathrm{h})^{-2}$ during the four days before arrival, and **(c)** a given percentage of trajectories traveling south of 10°N and remaining at pressure levels > 300 hPa within the ten days before arrival. Data: ERA5.

ERA5 representativeness (relative humidity): In Fig. S1.3 the relative humidity from the ERA5 pseudo-soundings are compared to the measurements of the radio soundings (Stephans et al., 2020) launched from the BCO and four research vessels, i.e., R/V RonBrown, R/V Meteor, R/V MS-Merian, and R/V Atalante. It illustrates that ERA5 agrees with the variability of the BCO sounding, while the soundings show higher saturation than ERA5. Further, we note that the deep saturated layer on 22 January 2020 was a local feature, not observed (or temporally delayed) on the remaining platforms. The mid-level cloud layer on 14 February, however, was a mesoscale feature, appearing in the observations of all platforms.

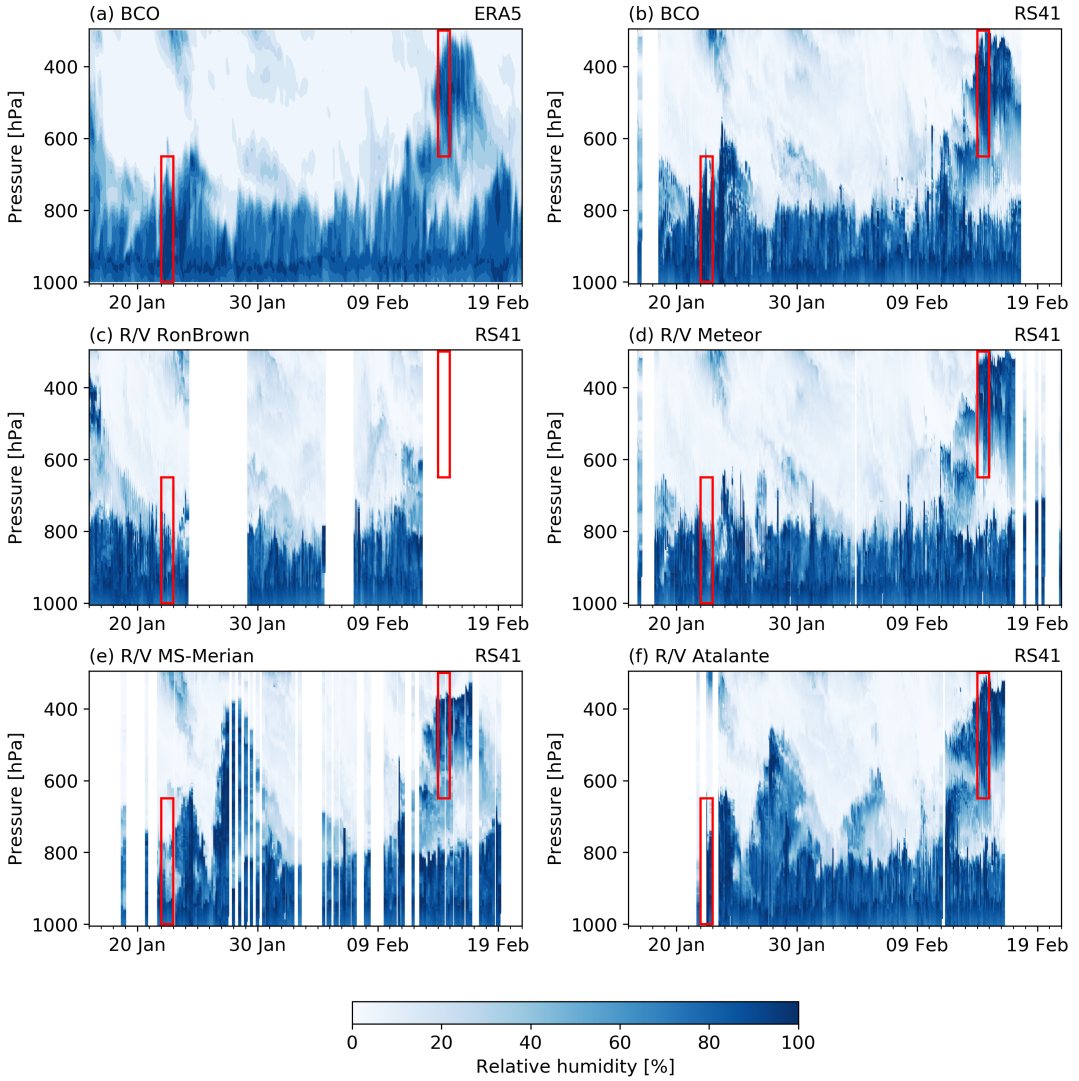

Figure S1.3: Comparison between **(a)** the ERA5 pseudo-soundings from the BCO and the measured atmospheric soundings launched from the **(b)** BCO, **(c)** R/V RonBrown, **(d)** R/V Meteor, **(e)** R/V MS-Merian, and **(f)** R/V Atalante from 16 January to 20 February 2020. The red boxes indicate the two case study days 22 January and 14 February 2020. Note that the R/V MS-Merian and R/V-Atalante spent much of the time south of the BCO.

ERA5 representativeness (wind fields): In Fig. S1.4, the horizontal wind fields of ERA5 are compared to the ones measured by the BCO soundings. The two data sets show an excellent agreement. Minor differences arise due to the temporal resolution, which is much higher for the measurements than for ERA5. Fig. S1.5 shows that the vertical velocities of the ERA5 trajectories (calculated based on ERA5's three-dimensional wind fields) is within the range derived from circular dropsonde measurements conducted in previous field experiments (George et al., 2021).

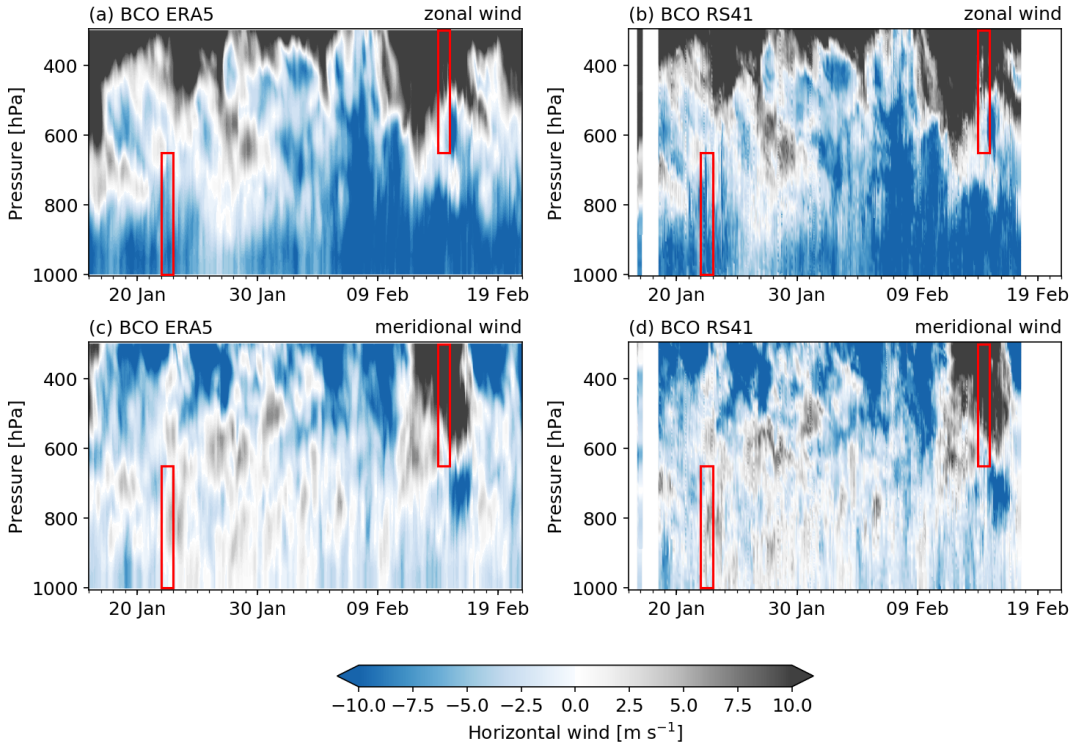

Figure S1.4: Comparison between the zonal/meridional wind component **(a/c)** from ERA5 pseudo-soundings from the BCO and **(b/d)** the measured atmospheric soundings launched from the BCO from 16 January to 20 February 2020. The red boxes indicate the two case study days 22 January and 14 February 2020.

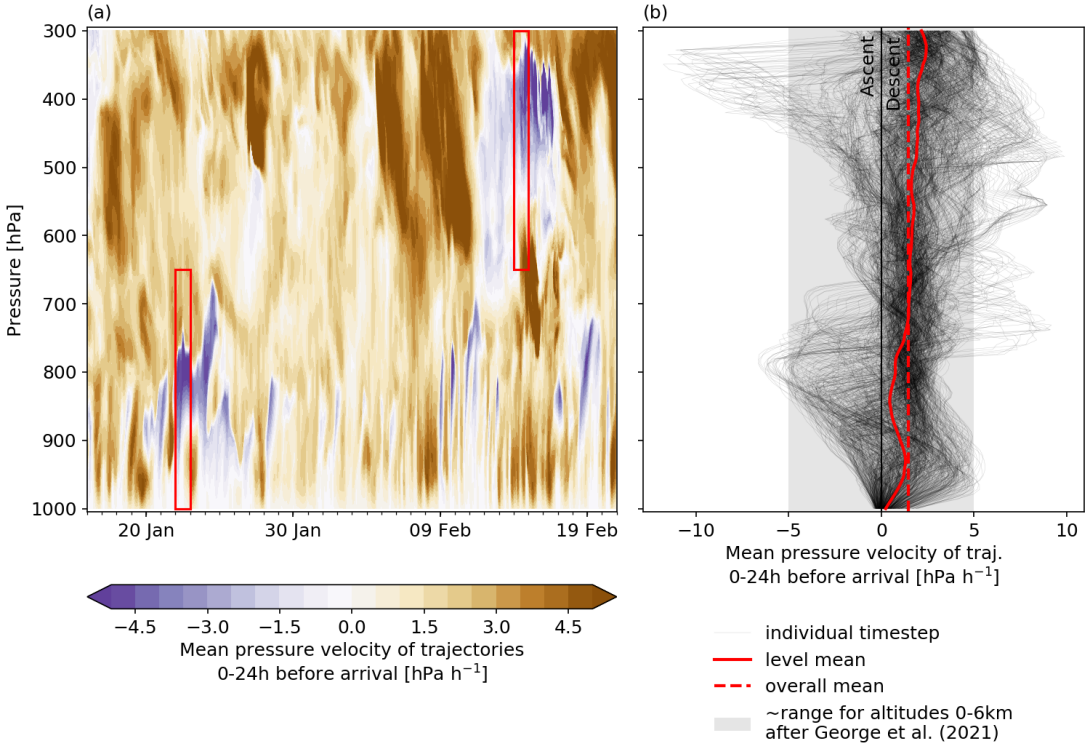

Figure S1.5: Mean pressure velocities derived from the backward trajectories started above the BCO during the last 24 h before arrival as **(a)** time series from 16 January to 20 February 2020, and **(b)** individual vertical profiles per time step (black thin lines), the mean over all time steps per pressure level (red continuous line) and the overall mean (red dashed line). The pressure velocity range determined by George et al. (2021), valid for altitudes 0-6 km, is indicated (gray shading).

ERA5 representativeness (daily means): The time series of the daily mean values of the variables shown in Fig. 3 of the paper, are shown in Fig. S1.6. The Pearson correlation between the ERA5 and the corresponding measurements and the mean difference between the two data sets are given in Table S1.1. ERA5's representativeness is excellent for IWV, good for CRE (except for a systematic bias towards lower values), and limited for precipitation and total ice water. Nevertheless, except for the minimum CRE over the domain (Fig. S1.6f) on 22 January 2020, all peaks/dips characterising the two case studies (22 January and 14 February 2020) in ERA5 are also present in the measurements. Note that the total ice water from CERES is not particularly informative, because it is based on many missing values (see paper for details).

Table S1.1: Pearson correlation coefficients and mean differences between daily means (or sums in the case of precipitation) from ERA5 and from measurements (as shown in Fig. S1.6) at the BCO or in Barbados' vicinity for the period 16 January to 20 February 2020.

	Correlation (ERA5, measurements)	Mean difference (ERA5 - measurements)
$IWV_{650\text{-}300\,hPa}$	0.97	-0.17 mm
$IWV_{1000\text{-}650\,hPa}$	0.93	-1.82 mm
Precipitation	0.47	-0.13 mm
total ice water	0.57	-26.66 $g\,m^{-2}$
CRE_{BCO}	0.68	-3.99 $W\,m^{-1}$
CRE_{domain}	0.6	-11.55 $W\,m^{-1}$

ERA5 representativeness (clouds): Fig. S1.7 and S1.8 show the mesoscale cloud pattern observed by MODIS Terra and Aqua and the CRE (including cloud phase information) from ERA5 and CERES for two exemplary time steps (night- and daytime) for each of the two case studies. The cloud band (Fish) with adjoining cloud free regions on 22 January 2020 is reproduced by ERA5. The horizontal width of the cloud bands and the associated daytime cooling, however, is larger and stronger in ERA5 compared to CERES. The liquid cloud overestimation by ERA5 is very pronounced in the north-eastern part of the domain. During night, CERES even detects ice clouds and therewith associated cloud radiative warming which is absent in ERA5. The mesoscale cloud pattern is less well reproduced by ERA5 on 14 February than on 22 January 2020. In this case, ERA5 underestimates ice clouds and the associated night-time cloud radiative warming.

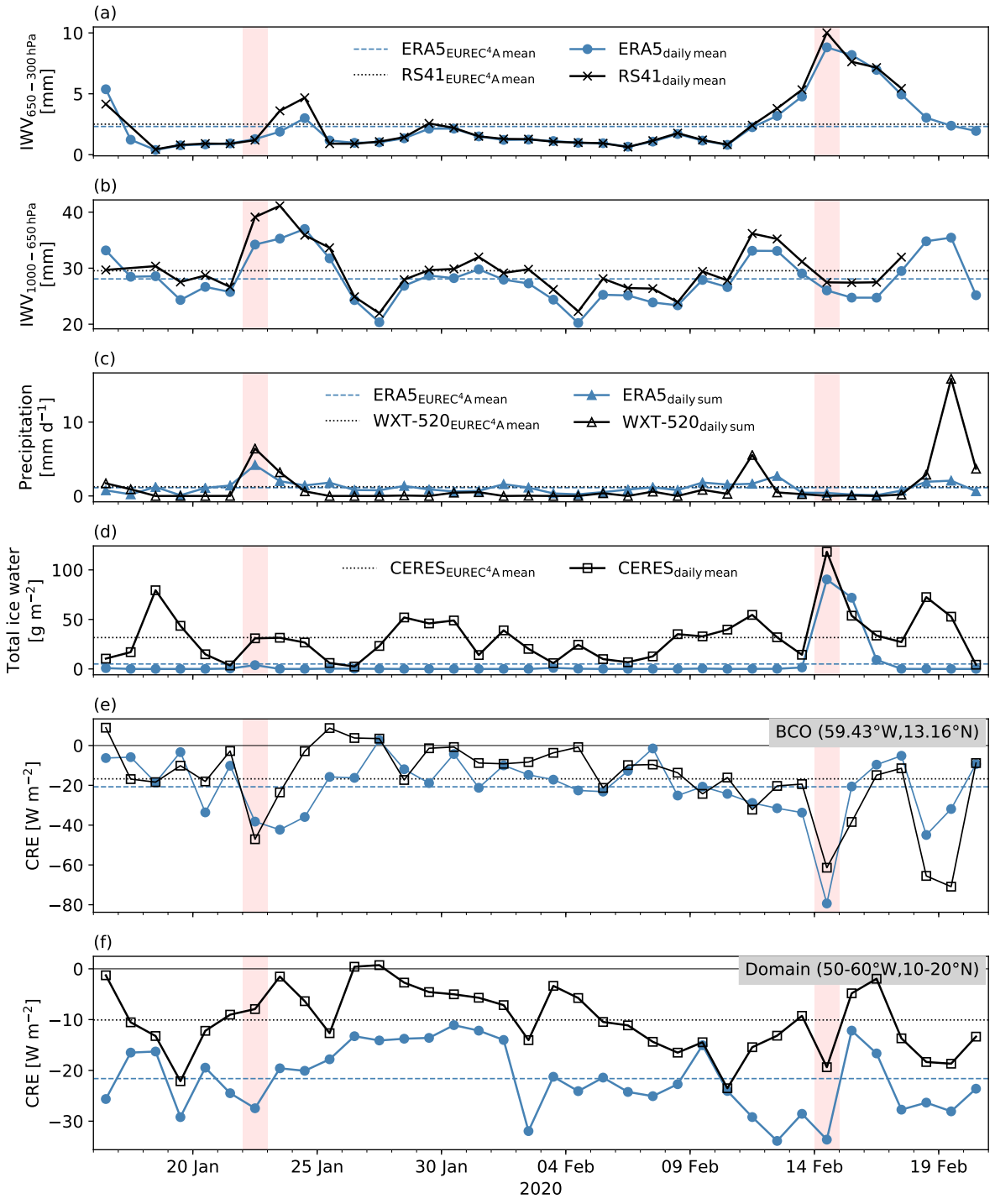

Figure S1.6: Comparison between daily mean values of **(a,b)** $IWV_{650\text{-}300\,hPa}$ and $IWV_{1000\text{-}650\,hPa}$ derived from the BCO soundings (RS41) and ERA5, **(c)** daily precipitation totals from the meteorological station (WXT-520) and ERA5, **(d)** total ice water from CERES and ERA5, **(e,f)** the net cloud radiative effect from CERES and ERA5. The values are shown for **(a-e)** the location of the BCO, and **(f)** as an area-mean over the domain $50-60°$ W, $10-20°$ N. The period of the two case studies, 22 January and 14 February, are indicated by the red shading. campaign mean values are shown dashed/dotted horizontal lines. The time axis is given in UTC (Barbados local time = UTC-4h).

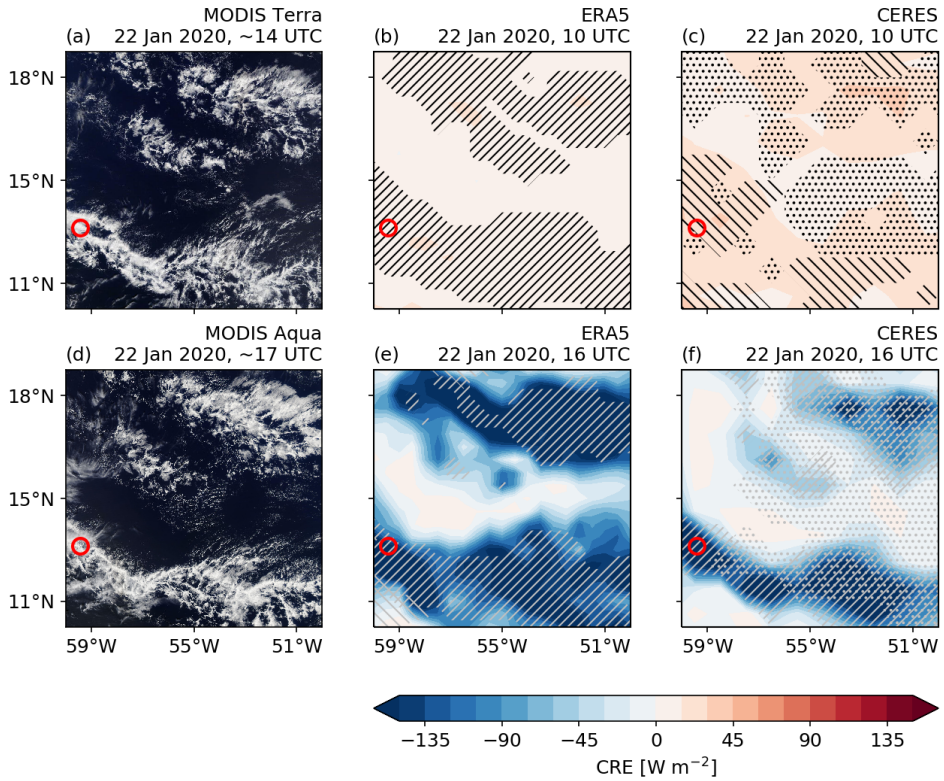

Figure S1.7: Mesoscale cloud organisation pattern as seen by **(a/d)** MODIS Terra/Aqua at ~14/17 UTC, and the CRE (shading) during local **(b/c)** night- (10 UTC) and **(e/f)** daytime in ERA5/CERES for 22 January 2020. Shown are also **(b,c,e,f)** total liquid water >50 g m^{-2} (right/forward tilted hatching), ; total ice water >5 g m^{-2} (left/backward tilted hatching), and **(c,f)** missing total ice water data (dotted area).

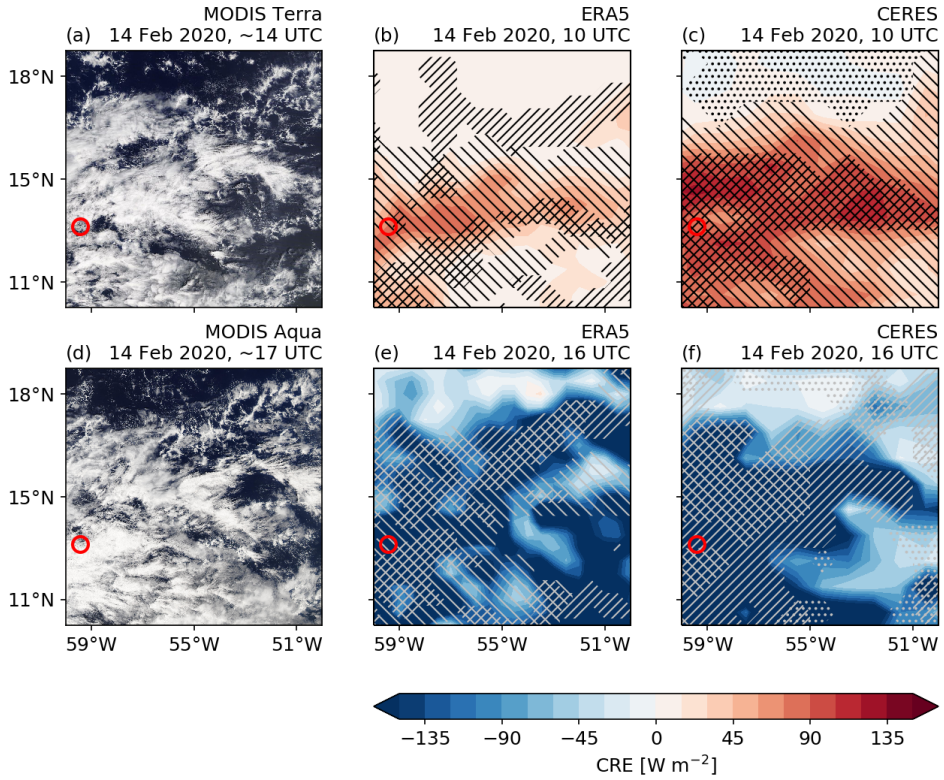

Figure S1.8: Similar to Fig. S1.7, but for 14 February 2020.